Extended Abstracts of the 2008 International Conference on Solid State Devices and Materials, Tsukuba, 2008, pp. 1102-1103

H-10-2

Graphene Nanoribbon Transistors and Resonant Tunneling Diodes

Gengchiau Liang[1], Hansen Teong[1], Kaitak Lam[1],
Neophytos Neophytou[2], and Dmitri E. Nikonov[3]
[1]Deparrtment of Electrical and Computer Engineering, National University of Singapore, Singapore;
Phone: +65-6516-2898 E-mail: elelg@nus.edu.sg
[2]School of Electrical and Computer Engineering, Purdue University, West Lafayette, Indiana 47907-1285
[3]Technology and Manufacturing Group, Intel Corp., SC1-05, Santa Clara, California 95052

1. Introduction

Graphene related materials have drawn a lot of attention from the device engineering community due to their unique electronic properties such as high carrier mobility, which makes them potential candidates for novel transistor channel materials. Carbon nanotube (CNT) FETs have been widely considered in this area, whereas the fabrication challenges and the chirality control of CNTs is a big drawback for their potential application in realistic device. Recent experimental studies [1-3] show the possibility to fabricate graphene nano-ribbons (GNR) transistors, and their potential as an alternative method to bypass the CNT chirality challenge while still retaining the excellent electronic properties of graphene sheets, such as high carrier mobility [4], which appear in the CNTs as well. Furthermore, the graphene sheet itself is a semi-metal and can be employed as the metal contacts. Similar to CNTs, the electronic structure of GNRs such as the bandgap (E_G), is a sensitive function of their width [5]. Additionally, quantum effects such as quantum tunneling dominate the OFF-current (I_{OFF}) of the device and strongly depend on the E_G, *i.e.*, the GNR width. Therefore, the dependence of the device behavior on the GNR width needs to be properly investigated for a rigorous treatment of the I_{OFF} of the device. In addition to transistor type devices, another potential application of GNRs in resonant tunneling diodes (RTDs) is also studied in this work due to the possibility to pattern GNRs in the different width [3] to form heterostructures.

2. GNR transistors

In the first part, we utilize a full real-space quantum transport simulator based on the Non-equilibrium Green's Functions (NEGF) approach self-consistently coupled to a 3D Poisson's solver for treating the electrostatics [6]. Using this model, the ballistic performance of double-gate armchair GNR (AGNR) MOSFETs and AGNR Schottky barrier (SB) FETs with different types of the contacts and regular metal with a constant density of states is evaluated. The details of the device structure are shown in Fig.1. Fig.2 (a) and (b) show the transfer characteristics AGNR MOSFETs and SB FETs, respectively with different width. Unlike conventional Silicon based planar MOSFETs, the performance of AGNR FETs depends on their widths. It is because the bandgap of AGNRs caused by the quantum confinement effects, cf., Table I. Furthermore, the width dependency of the device performance of these different types of AGNR FETs, in terms of the subthreshold swing (SS), the drain-induced-barrier-lowering (DIBL), the ON-current, the switching delay (τ), and the power-delay-product (PDP), are investigated. Our simulation results show that the device performance is limited by the tunneling currents which depend on E_G, and hence on AGNR width. As shown in Fig. 3 and Fig. 4, among these different transistor types, AGNR MOSFETs (with infinite semiconducting contacts) always have the best performance.

3. GNR RTDs

Due to the spatial quantum confinement, the bandgap of an AGNR is a function of its width. As AGNR width increases, the bandgap decreases. Therefore, a double barrier band structure can be achieved by controlling the widths of AGNRs as shown in Fig. 5 and quantum states can be generated between the barriers. The current-voltage (I-V) characteristics of such AGNR RTD are then investigated using NEGF approach and the result shows the standard RTD behavior with the negative differential resistance (NDR) effects. To further understand the mechanism of NDR effects, the calculated transmission as a function of applied bias, T(E,V) through the AGNR RTD is shown in Fig 6(b). The transmission peak of the AGNR RTD shifts under bias and disappears when it reaches the conduction band edge (E_C) of the contact. The cross points present the bias points at the corresponding I-V curve in (a). Therefore, as the energy state drops into the bandgap region, the tunneling current is cut off and hence the NDR effect is observed. Due to the high mobility of AGNR, the peak current density can reach 5kA/cm^2 at low temperature.

4. Conclusions

In summary, we present the theoretical study of width effects in AGNR MOSFETs and SBFETs with both regular metal contacts and graphene semi-metal contacts, and examine the possibility of implementing AGNR as RTDs. A full real-space quantum transport simulator is used for our simulations. Due to the dependence of the electronic structure of AGNRs on their width, the device performance of these three types of transistors shows strong width dependence, especially on the quantum tunneling current such as BTBT in MOSFETs and ambipolar conduction in SB FETs. Overall, the device performance improves as the device width reduces. Moreover, by controlling the widths of ANGRs, heterostructure with double barriers can be constructed. The currents through such structure show the standard RTD behavior which is shown to be modulated by the AGNR width and applied bias.

References

[1]C. Berger, et al., *Science*, **312**, 1191, 2006.[2]M. C. Lemme, et al., *IEEE Electronic Device Letters*, **28** (4) 282, 2007. [3]Xiaolin Li, et al., Science 319, 1229 (2008).[4]B. Obradovic, et al., *Appl. Phys. Lett.*, **88**, 142102, 2006. [5]GC. Liang, et al., *IEEE Trans. Electron. Devices*, **54** (4), 677, 2007. [6]G. C. Liang,et al. , *J. Appl. Phys.*, **102**, 054307, 2007.

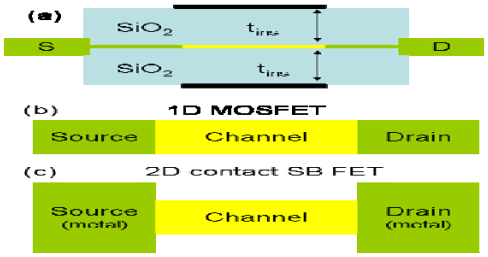

Fig. 1: (a) A schematic of the simulated dual-gate graphene nanoribbon MOSFETs. The oxide thickness (t_{ins}) is 1 nm and the channel length is 12.5nm. (b) Top view of (a) for a 1D MOSFET. The source, channel and drain parts are composed by the same width armchair GNRs. The source and drain are heavily doped nanoribbon contacts while the channel is undoped. (c) Top view of (a) for a SB MOSFET. The normal metal contacts with the constant density of states are used, and their impact on the device is investigated.

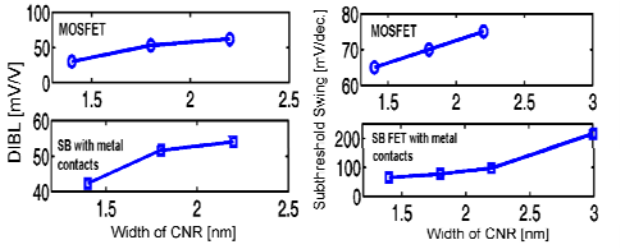

Fig. 3: Width dependence (for different types of GNR FETs) of the device performance: subthreshold swing (*SS*) and drain-induced-barrier-lowering (*DIBL*). Due to the fact that the bandgap of GNRs is the function of their width, both of the *SS* and *DIBL* degrade as the width of GNR increases. Among these two types of devices, GNR MOSFETs always have the best performance because band-to-band tunneling occurs at a large negative bias. For SB FETs, however, the ambipolar conduction can dominate the total current when Vg is smaller than half of the V_{DS}, and degrades the device performance of the SB FETs.

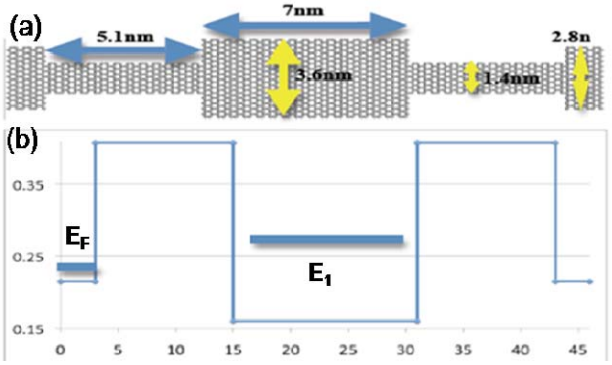

Fig. 5: (a) Simulated RTD structure with semi-infinite 2.8nmwide AGNR as the contacts. (b) Schematic band diagram (E_C) of the simulated AGNR RTD as shown in (a). E_1 presents the quantum state formed by the double barriers.

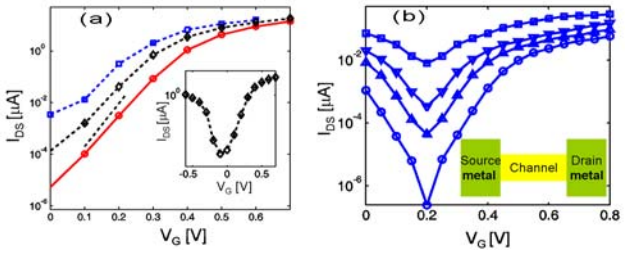

Fig. 2: (a) Simulated current I_{DS} vs. V_{GS} for a 12.5 nm long channel 1D armchair GNR MOSFETs (Fig. 1b) with 1.4 nm width (circle), 1.8 nm (diamond), and 2.2 nm width (square) at V_{DS}=0.4V. The dashed line presents the ideal subthreshold swing at room temperature (60 mV/decade). The inset shows the transfer performance of the second case for the large V_G window. Band-to-band tunneling occurs at the negative bias side. (b) I_{DS} vs. V_{GS} of the SB armchair GNR FETs with 1.4 nm width (circle), 1.8 nm (up-triangle), 2.2 nm (down-triangle) and 3.0nm width (square) at V_{DS}=0.4V using the regular metal as the contacts. The ambipolar conduction plays an important role in the *OFF*-state.

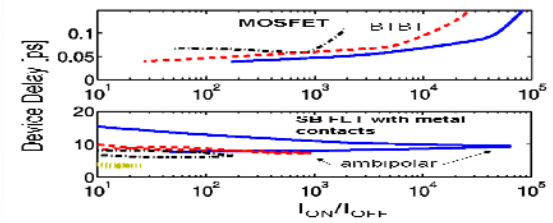

Fig. 4: Device switching delay (τ) at V_{DD}=0.4 V for the two different types GNR FETs with various widths: 1.4nm (solid blue line), 1.8nm (dashed red line), 2.2nm (dashed-dot black line) and 3.0nm (dot green line). Before tunneling current starts to play an important role in the total current, the device delay does not depend on the device size. However, when tunneling currents start dominating the total currents, the device delay strongly depends on the size of devices because tunneling is stronger in smaller bandgap (larger width) devices.

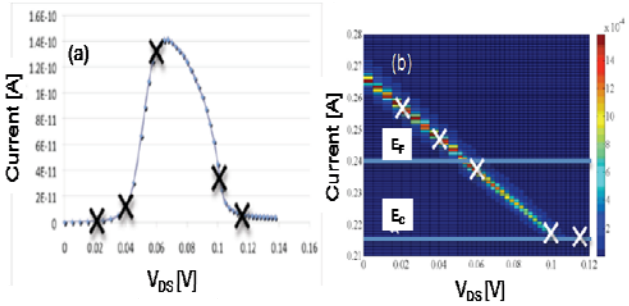

Fig. 6: (a) Simulated I-V characteristics of an AGNR RTDs whose device structure is shown in Fig. 5, based on the real space, π-orbital tight-binding NEGF simulations. It resents the standard RTD behavior with NDR effects under the low bias. (b) Calculated transmission T(E, V) (color plot) through the AGNR RTD, its transmission peaks shift under bias and disappear when they reach the conduction band edge E_C. The cross points present the bias points at the I-V curve in (a)

Table 1: Calculated bandgap energy of the armchair GNR with the different widths using the simple π-orbital tight-binding model.

	Width of armchair GNRs			
	1.4 nm	1.8nm	2.2nm	3.0nm
E_G [eV]	0.8	0.66	0.56	0.42